Vision Research 160 (2019) 24–36

Contents lists available at ScienceDirect

Vision Research

journal homepage: www.elsevier.com/locate/visres

Growing tiny eyes: How juvenile jumping spiders retain high visual performance in the face of size limitations and developmental constraints

John T. Goté[a], Patrick M. Butler[a], Daniel B. Zurek[a,b], Elke K. Buschbeck[b], Nathan I. Morehouse[a,b,*]

[a] Department of Biological Sciences, University of Pittsburgh, Pittsburgh, PA, USA
[b] Department of Biological Sciences, University of Cincinnati, Cincinnati, OH, USA

ARTICLE INFO

Keywords:
Visual ecology
Salticidae
Allometric scaling
Developmental morphology
Eye development
Visual performance

ABSTRACT

Adult jumping spiders are known for their extraordinary eyesight and complex, visually guided behaviors, including elaborate communicatory displays, navigational abilities, and prey-specific predatory strategies. Juvenile spiders also exhibit many of these behaviors, yet their visual systems are many times smaller. How do juveniles retain high visually guided performance despite severe size constraints on their visual systems? We investigated developmental changes in eye morphology and visual function in the jumping spider *Phidippus audax* using morphology, histology, ophthalmoscopy, and optical measurements. We find that juvenile spiders have proportionally larger lenses in relation to their body size than adults. This should alleviate some of the costs of small body size on visual function. However, photoreceptor number in the anterior lateral eyes (ALE) remains constant from early development onward, consistent with a developmental constraint on photoreceptor differentiation. To accommodate these photoreceptors within the diminutive volume of the spiderling cephalothorax, ALE rhabdoms in early life stages are more tightly packed and significantly smaller in diameter and length, properties that expand across development. Lens focal lengths increase as eyes and retinas grow, resulting in a remarkable maintenance of ALE spatial acuity and field-of-view across life stages. However, this maintenance of acuity comes at a sensitivity cost given the small rhabdomal volumes required by space constraints early in life. Taken together, our results indicate that young jumping spiders have eyes already equipped for high acuity vision, but these young spiders may struggle to perform visually demanding behaviors in low-light environments, a notion that warrants further testing.

1. Introduction

The visual systems of jumping spiders (family Salticidae) are among the most sophisticated in the Arthropoda (Harland, Li, & Jackson, 2012; Homann, 1928; Land, 1985b; Morehouse, Buschbeck, Zurek, Steck, & Porter, 2017). Composed of four pairs of single-lens eyes, these modular visual systems provide a range of exceptional visual functions, especially given their small size. For example, the large forward-facing anterior median eyes (AMEs, also called the 'principal eyes') are typically less than 500 μm in their longest dimension at adulthood, and yet they provide color vision (Zurek et al., 2015), depth perception (Nagata et al., 2012), a moveable 'gaze' (Land, 1969a), and spatial acuity equal to or surpassing that of a pigeon or domestic cat (e.g., with interrhabdomal angles of 0.04–0.11°, Harland et al., 2012). The AME's remarkable acuity is the product of a paired-lens system that magnifies focused images on the underlying tiered and densely packed photoreceptor mosaic (Williams & McIntyre, 1980). The smaller-lensed, forward-facing anterior lateral eyes (ALEs) and rear-facing posterior lateral eyes (PLEs) provide a nearly 360° combined field-of-view. These so-called 'secondary eyes' offer monochromatic vision at a slightly lower resolution that nevertheless rivals some of the best acuities found in insect visual specialists (e.g., 0.4°, roughly equivalent to dorsal-facing acuity of a *Sympetrum* dragonfly 10–20 times a jumping spider's size, Labhart & Nilsson, 1995). The larger rhabdoms of the ALE and PLE are more light sensitive than those of the AME, allowing them to offer hyperacute motion detection (Zurek & Nelson, 2012b) in the visual periphery. The dorsal-facing posterior medial eyes (PMEs) add coarse-resolution detection of overhead objects such as looming predators for

Abbreviations: A, adult; ALE, anterior lateral eye; AME, anterior medial eye; EJ, third instar, early juvenile; H, hatchling; IRD, interrhabdomal distance; LJ, fourth through sixth instars, late juvenile; PLE, posterior lateral eye; PME, posterior medial eye

* Corresponding author at: Department of Biological Sciences, University of Cincinnati, Cincinnati, OH 45221-0006, USA.
E-mail address: nathan.morehouse@uc.edu (N.I. Morehouse).

https://doi.org/10.1016/j.visres.2019.04.006
Received 17 March 2019; Received in revised form 18 April 2019; Accepted 18 April 2019

some groups of jumping spiders (Land, 1985a).

Not surprisingly, jumping spiders exhibit behavioral repertoires with complexity rivaling that of their visual systems. For example, jumping spiders are cursorial predators, relying on their ability to track and capture prey (Jackson & Pollard, 1996). This can involve the use of sophisticated route detouring (Tarsitano & Andrew, 1999; Tarsitano & Jackson, 1997), counting/numerical competence (Cross & Jackson, 2017; Nelson & Jackson, 2012b), prey-specific predatory strategies (Jackson & Pollard, 1996; Jackson & Wilcox, 1990; Nelson & Jackson, 2011), and learned and/or innate preferences that help to identify toxic (Taylor, Amin, Maier, Byrne, & Morehouse, 2016; Taylor, Maier, Byrne, Amin, & Morehouse, 2014) or particularly profitable prey (e.g., blood-filled mosquitoes, Jackson, Nelson, & Sune, 2005; Nelson & Jackson, 2012a). When navigating their surroundings, jumping spiders are able to return to overnighting nest sites with the help of beacon-nest associative learning in both real (Hoefler & Jakob, 2006) and virtual environments (Peckmezian & Taylor, 2015). Male jumping spiders also famously engage in elaborate courtship displays to females (Clark & Uetz, 1993; Elias, Maddison, Peckmezian, Girard, & Mason, 2012; Girard, Kasumovic, & Elias, 2011; Lim, Li, & Li, 2008; Taylor & McGraw, 2013), and ritualized contest displays to rival males (Lim & Li, 2004). Both sexes often engage in complex intraspecific signaling, a phenomenon particularly prominent in ant-mimicking jumping spiders who must distinguish themselves from their ant models when interacting with conspecifics (e.g., Nelson & Jackson, 2007).

Many of the complex behaviors described above can also be found in juvenile spiderlings. For example, Nelson, Jackson, and Sune (2005) found that *Evarcha culicivora* spiders adopt prey-specific hunting strategies as juvenile spiderlings, a phenomenon that has since been observed in other jumping spider species (e.g. *Yllenes arenarius*; Bartos, 2008; Bartos & Szczepko, 2012). Similarly, color biases in foraging preferences were found in both adult and juvenile *Habronattus pyrrithrix* (Taylor et al., 2014). Although courtship displays are restricted to sexually mature adults, intraspecific communicatory displays are by no means adult-limited, with complex display repertoires observed in juveniles in a variety of species (e.g., *Servaea incana*, McGinley, Mendez, & Taylor, 2015).

Observations of sophisticated, visually guided juvenile behaviors suggest that juveniles may have visual abilities similar to those of their adult counterparts. However, the cephalothorax volume of early juvenile stages is a fraction of its adult size, often by an order of magnitude or more (Taylor & Peck, 1975). This should impose severe space constraints on their developing visual systems. Because many visual functions can be strongly impacted by reductions in eye size (e.g., sensitivity, field of view, spatial acuity), this presents something of a puzzle: How do juvenile jumping spiders seemingly retain visual functionality across ontogeny despite extreme space limitations? Almost nothing is known about how jumping spider visual systems change across development, with the exception of a series of early studies on the development of AME retinal tiering in first instar spiderlings (Blest & Carter, 1987, 1988; Blest, 1988; see also Fenk, Heidlmayr, Lindner, & Schmid, 2010 for work on lens growth in the ctenid spider *Cupiennius salei*). Here, we characterize changes in a variety of visual system traits across development, from egg-sac emergence (2nd or 3rd instar) to adulthood, focusing primarily on the ALE of the jumping spider *Phidippus audax* (Fig. 1).

Research on eye allometry and development in other systems provides us with a number of working hypotheses for how jumping spiders might address the challenges associated with retaining visual function across development. First, juveniles in other animal groups often protect some level of visual functionality by beginning development with proportionately larger eyes in relation to body and/or head size. This is especially common in vertebrate camera eyes, which tend to exhibit disproportionately large sizes during early juvenile stages (e.g., fish, Fernald, 1985; geckos, Werner & Seifan, 2006; giraffes, Mitchell, Roberts, van Sittert, & Skinner, 2013; primates, Augusteyn, Maceo Heilman, Ho, & Parel, 2016; sharks, Harahush, Hart, Green, & Collin, 2009), a phenomenon so common that we cognitively associate it with youthfulness in our own species (Berry & McArthur, 1986) and select for it in domesticated (Waller et al., 2013) and fictional animals (Hinde & Barden, 1985; Morris, Reddy, & Bunting, 1995). This developmental strategy directly alleviates some of the costs of small body size on visual function, and can also be found in static allometries among adults within and across species (Augusteyn, 2014; Howland, Merola, & Basarab, 2004; Rutowski, Gislen, & Warrant, 2009). However, juvenile head size still constrains the maximize size of a juvenile eye, and thus eyes must still grow. The result is a characteristic pattern of negative ontogenetic allometry, where disproportionately large juvenile eyes grow more slowly than other body structures, eventually reaching their proportional adult size. We predicted that jumping spider eyes would exhibit such negative ontogenetic allometry, beginning juvenile development at proportionally larger sizes in relation to cephalothorax width.

Regardless of whether jumping spider eyes grow with negative allometry, it is clear from casual observation that their lenses get larger across development (Fig. 1, see also Fenk et al. (2010) for lens growth in the non-salticid *C. salei*). However, nothing is known about growth of internal structures, including photoreceptor proliferation and changes to retinal mosaic dimensions. Here, there are a number of precedents in the animal kingdom. In vertebrates, retinas expand with eye growth, but taxa differ in how this retinal growth is accomplished. In mammals, photoreceptor proliferation ceases around the time of birth, with subsequent increases in retinal size accomplished via expansions in retinal cell size and spacing (Kuhrt et al., 2012). In contrast, other vertebrate taxa such as fish and amphibians continue adding photoreceptors across development alongside expansion of the size and spacing of existing retinal mosaic cells, with new photoreceptors appearing in a germinal zone along the retinal margin (Fernald, 1985).

Although either of these modes of retinal growth (i.e., continued photoreceptor proliferation and/or retinal cell expansion without proliferation) could in principle occur during jumping spider eye development, it is worth considering these two possibilities in light of how eye growth occurs in other arthropods. Recent work to describe the molecular basis of spider vision (reviewed in Morehouse et al. (2017)) revealed substantial overlap in the genes expressed during spider eye development and those known to form the retinal determination network for insect compound eyes and ocelli. These results, combined with morphological and phylogenetic considerations, has led to the proposition that spider secondary eyes (ALE, PLE, PME) were derived from an ancient pair of lateral compound eyes, whereas the 'principal' eyes (AME) were derived from ancient medial ocellar eyes (Morehouse et al., 2017; Schomburg et al., 2015). If true, this would suggest that mechanisms of eye growth in insect compound eyes might apply to retinal growth in spider eyes.

Of particular relevance in this context is the timing of photoreceptor differentiation: in insects, photoreceptor differentiation precedes lens development (Charlton-Perkins & Cook, 2010; Kumar, 2012; Tsachaki & Sprecher, 2012). After the lens system is added to the top of an ommatidial unit, photoreceptor additions to that ommatidium are no longer possible, and subsequent photoreceptors must be added as part of a new ommatidial unit (Kumar, 2012). Eye growth in ametabolous and hemimetabolous insects is therefore accomplished via ommatidial addition along an anteroventral proliferation zone (Friedrich, 2006). Interestingly, this pattern of halted photoreceptor differentiation following lens production also holds for larval eyes in the holometabolous diving beetle, *Thermonectus marmoratus* (Werner & Buschbeck, 2015), despite dramatic increases in the size of these tubular single lens eyes across larval instars. *T. marmoratus* larval eyes are also thought to derive from an ancestral compound eye (Liu & Friedrich, 2004; Stahl, Baucom, Cook, & Buschbeck, 2017), making them an interesting evolutionary analogue for spider eyes. Because the spider lens system is added to the eye in the final stages of embryonic development, spider

Fig. 1. Composite image representing the major difference in body size observed between a *Phidippus audax* adult female (above) and one of her newly hatched spiderlings (below).

retinas may be constrained to embarking upon post-embryonic development with their full complement of photoreceptors. This would thus favor an expectation of retinal growth via cell expansion alone, analogous to mammalian retinal development. Preliminary evidence indicates that this may be the case for the principal eyes (Blest & Carter, 1987), but nothing is known about the secondary eyes. Based on these considerations, we hypothesized that photoreceptor differentiation would occur only during the embryonic phase, with post-embryonic retinal growth occurring strictly through increases in the size and spacing of the existing photoreceptor complement.

Several visual system properties rely on careful coordination of the size and spatial positioning of lenses and retinas. For example, to receive the sharpest image provided by the visual optics, a retina must be positioned at the appropriate distance from the lens (or alternatively, the focal distance of the lens must be adjusted to match the position of the retina). Organismal groups with single lens eyes differ in how this is accomplished over development. For example, juvenile vertebrates often do not begin post-embryonic development with eyes sharply focused at infinity (emmetropic), but rather start either hyperopic (far-sighted) or myopic (near-sighted) and achieve emmetropia later in development (Hofstetter, 1969; Wallman & Winawer, 2004). This is accomplished through changes to the vitreous-humor-filled distance between the lens and retina (e.g., in guinea pigs, Howlett & McFadden, 2007) and/or the size and power of the lens itself (e.g. in mice, Schmucker & Schaeffel, 2004). This process of developmentally "focussing" the eye can include both passive changes and homeostatic processes shaped by visual feedback during development (Flitcroft, 2014; Mark, 1972). Far less is known about invertebrate camera eyes, but a recent study by Werner and Buschbeck (2015) revealed surprisingly rapid re-establishment of emmetropia following instar molts in the camera-type eyes of diving beetle larvae, a process potentially aided by rapid uptake of water to the vitreous-filled eye tube. Nothing is known about how this is controlled in spider eyes across development, but from a functional standpoint, we might expect careful maintenance of emmetropia across instars through adjustments to the vitreous body and/or focal length of the lens.

Changes in the size and position of the retina can also induce changes in an eye's field of view and/or spatial acuity. For example, in the cichlid fish *Haplochromis burtoni*, adjustments to the size and position of the retina in relation to the lens result in the preservation of the eye's field of view across development (~181° solid angle, Fernald, 1985). However, because these fish continue to add photoreceptors to their retinas, the result is an increase in visual acuity across development from 6.9 cones per degree in small juveniles to 14.8 cones per degree in larger fish (Fernald, 1985). Such increases in visual acuity with ontogenetic eye growth appear common in fish (Hairston, Li, & Easter, 1982; Miller, Crowder, & Rice, 1993). Other outcomes are also possible, however, including an expansion of the field of view with no change in visual acuity and/or combined changes in field of view and acuity. For example, in the squid *Sepia officinalis*, acuity increases across development as a result of changes to lens optics (squid retinas do not add photoreceptors during post-embryonic development, Groeger, Cotton, & Williamson, 2005), presumably resulting in a decrease in field of view. In contrast, in the giraffe, both field of view and acuity are maintained across ontogeny, although changes to cranio-facial structure result in increased binocular overlap in adults (Mitchell et al., 2013). Again, nothing is known about how the field of view and spatial acuity of spider eyes changes, if at all, across development.

To investigate whether spider eyes exhibit a pattern of negative allometry by beginning juvenile development with disproportionately larger lenses, we first measured the ontogenetic allometry of lens sizes for all four eye pairs as compared to cephalothorax width in the jumping spider *Phidippus audax*. We then used a custom made micro-ophthalmoscope (Stowasser, Owens, & Buschbeck, 2017) to fully map all photoreceptors of the ALE retina *in vivo* across a series of developmental stages from newly hatched spiderlings to adults. This allowed us to evaluate directly whether jumping spiders add photoreceptors progressively during ontogeny, or begin post-embryonic development with their full complement of photoreceptors. To investigate changes to photoreceptor size and shape, we used histological measurements of

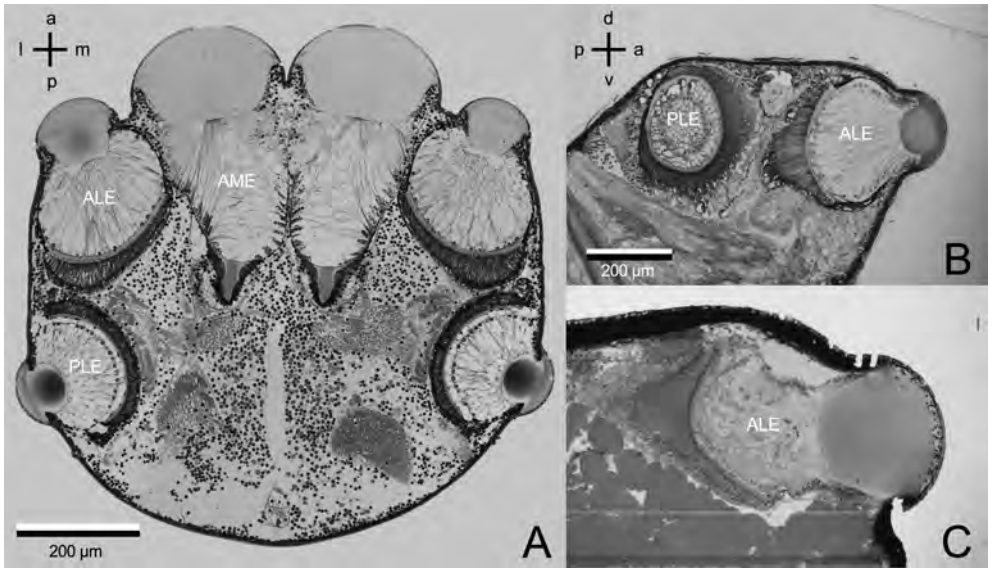

Fig. 2. (A) Transverse (horizontal) section of a hatchling jumping spider with eye pairs annotated in the vitreous body between the lens and retinal structures (AME; anterior medial eye, ALE; anterior lateral eye, PLE; posterior lateral eye). (B, C) Sagittal sections displaying size comparison between early juvenile (B) and adult ALE retinas (C). Body axes are labeled as follows: anterior (a), posterior (p), lateral (l), medial (m), dorsal (d), and ventral (v). The scale bar in panel B also applies to panel C.

retinal cross sections from two sectioning planes (transverse and sagittal) to quantify the length, diameter, spacing, and approximate volume of photoreceptor rhabdoms at different developmental stages (Fig. 2). We then employed micro-ophthalmoscopic measurements to monitor developmental changes to functional properties of the whole ALE, including the eye's field of view and spatial acuity. Finally, we used optical techniques to measure changes in lens focal lengths across developmental stages. In combination, these studies provide the first glimpse into how spider vision changes across development at morphological and functional levels.

2. Methods

2.1. Study species and animal care

Phidippus audax (Hentz, 1845) is a large jumping spider common to grasslands, open woodlands, and human-disturbed habitats across North and Central America (Taylor & Peck, 1975). Experimental animals were either field-collected or were the F1 offspring of field-collected individuals. Spiders were collected in the warm months of 2015 and 2016 from two field sites: an agricultural site in Rochester, PA (Kretschmann Family Organic Farm, 40°44′44.4″N 80°09′49.0″W) and a recreational site within a municipal park (Frick Park, 40°25′48.8″N 79°54′01.7″W).

Following field collection, spiders were maintained in the laboratory either in climate-controlled chambers or a specialized rearing room with a consistent photoperiod (16 h:8 h, light:dark) and a constant temperature (chambers: 24 °C; rearing room: 22–24 °C). Spiders were individually housed in clear plastic containers, with water provided to juvenile spiders via dental wicks connected to small water reservoirs. Spiders were fed twice weekly with cricket nymphs (instars 1–3 of *Acheta domesticus* or *Gryllodes sigillatus*). Total cricket mass for each feeding was approximately twice the mass of the specific spider. For spiders that were F1 offspring of field-caught individuals, egg sacs were monitored for signs of spiderling emergence (typically in the second instar), and separated into individual containers once the majority of an egg sac had emerged.

2.2. Measurement of external morphology across development

We quantified developmental changes in external morphology, including cephalothorax width and lens diameters, by taking photographs of the dorsal surface of live spiders using a stereomicroscope and calibrated imaging system (Leica M205C with DFC450 camera, Leica Application Suite software, version 4.1.0, Leica Microsystems Ltd., Heerbrugg, Switzerland). Animals were lightly anaesthetized using carbon dioxide prior to imaging to help reduce movement. Coordinates of morphological landmarks were identified using ImageJ (version 1.49, Abramoff, Magalhaes, & Ram, 2004). We then used a MATLAB script to calculate linear distances between landmarks. Using this method, we measured lens diameters of the anterior medial eyes (AMEs), anterior lateral eyes (ALEs), and posterior lateral eyes (PLEs). The linear distance between the midpoint of the left and right PLE diameters was utilized as a proxy for cephalothorax width (CW). Lens diameters were measured as the linear distance between the two points where each lens intersected with the body profile. Left and right lenses were measured for each eye pair and then averaged, resulting in a single per-spider estimate of lens diameter, per eye type, per time point.

We measured lens diameters and cephalothorax widths of developing spiders from two cohorts of spiderlings. Measurements were conducted once per week starting at spiderling emergence from the egg sac and continuing until adulthood. The first cohort (n = 14) was composed of spiderlings from a single egg sac that hatched in April 2015. We measured a second cohort of spiders (n = 12) from eggs sacs laid by three field-caught females in June 2016. To assign instar numbers to individual spiders, we used two developmental criteria: emergence from the egg-sac, which occurs in either the second or third instar, and the significant increase in instar duration that begins with the fifth instar. The latter, first described by Taylor and Peck (1975), was readily identifiable post-hoc using individual developmental records, and allowed us to resolve any ambiguities about instar number arising from the variable timing of emergence from egg sacs. For our analysis of developmental allometries, we used these individual instars. However, in subsequent analyses, we combined instars into broader developmental stages (see Fig. A1) as follows: hatchling (H, second instar), early juvenile (EJ, third instar), late juvenile (LJ, fourth through sixth instars), and adult (A, sixth through ninth instars depending on timing of molt into adulthood).

Morphometric changes over development were analyzed using linear mixed-effects models implemented in R (version 3.5.1; R Core Team, 2018) using the package lme4 (version 1.1-15; Bates, Maechler, Bolker, & Walker, 2015). Models were fitted using restricted maximum likelihood, with degrees-of-freedom estimated using Satterthwaite's approximation. We examined increases in CW, AME, ALE, and PLE lens diameter across instars, as well as the influence of sex, cohort, and their interaction. We modeled spider identity as a random factor nested in cohort, and treated instar as a continuous variable. Tests of fixed effects

were accomplished using Type III sums-of-squares. The same methods were used to analyze relative eye size (lens diameter divided by CW).

2.3. Ophthalmoscopic measurements

2.3.1. Animal preparation and imaging

We imaged the AME and ALE retinas of live individuals using a micro-ophthalmoscope inspired by an earlier design developed by Land (1969a, 1969b). For an in-depth description, see Stowasser et al. (2017). Briefly, the micro-ophthalmoscope was composed of an optical path with two achromatic lenses (top lens: f = 150 mm, AC254-150-A; accessory lens: f = 200 mm, AC254-200-A; Thorlabs, Newton, NJ, USA) and a 10× objective (UPlanFl, Olympus, Central Valley, PA, USA). Epi-illumination was provided by a mercury light (ULH100HG and BX-RFA, Olympus), and digital imaging via a CMOS camera (ORCA-Flash 4.0V2 Digital CMOS, C11440-22CU, Hamamatsu, Hamamatsu City, Japan). Adjustments to the accessory lens position allowed for the ophthalmoscope to be focused across a range of depths inside the spider eye, enabling us to consistently image retinas despite changes to eye dimensions and focal length across development.

Spiders were temporarily anaesthetized with carbon dioxide and then mounted with beeswax onto a metal stick centered in a custom goniometer. Images of the retina were then taken by fine-positioning the spider so that the eye of interest was centered within the visual field of the ophthalmoscope and roughly in focus without the accessory lens. The accessory lens was then put in place with its position adjusted so that the retina was brought into sharp focus.

Because the field of view of the ALE far exceeds that of the ophthalmoscope, the generation of full ALE retinal maps required systematic collection and assembly of 40–60 images per eye. We did so by rotating and tilting spiders within the goniometer to produce a series of radial transects at 20° azimuthal increments extending from the center of the retinal field to the edges. Images were captured along these transects at 10° or 15° polar increments, starting at the center. Spiders were then removed from the goniometer, and either euthanized for use in other measurements (e.g., 'hanging-drop' measurements), or kept alive and re-imaged using the same methods four months later ($n = 7$). Three of these re-imaged spiders underwent an instar molt in the interim between measurements.

2.3.2. Quantification of photoreceptor numbers, spatial acuity, and field of view

We used the resulting sets of retinal images to quantify ALE photoreceptor number, spatial acuity, and field of view from individuals at different life stages. First, to count total photoreceptor numbers per retina, we merged all images from a retina into one large composite image by stitching the images together using the Photomerge function in Adobe Photoshop (Photoshop CC, Adobe, Inc., San Jose, CA, USA). We were able to construct full ALE retinal maps for 22 spiders from different developmental stages, including early juvenile (EJ; $n = 5$), late juvenile (LJ; $n = 6$), and adult stages (A; male $n = 6$, female $n = 5$). We were also able to construct full retinal maps for all re-imaged spiders ($n = 7$). We then used the multi-point tool in ImageJ to count individual rhabdoms from these composite images. Differences in photoreceptor number across developmental stages were investigated using a one-way ANOVA, while differences between time points for re-imaged spiders were tested using paired *t*-tests.

To measure spatial acuity and field of view, we worked with the original images rather than composite images, as the Photomerge function introduces small distortions to raw images when merging them. We measured these metrics in a total of 20 spiders (EJ; $n = 6$, LJ; $n = 6$, A; male $n = 5$, female $n = 3$), including two consecutive measurements from all re-imaged spiders ($n = 7$). We measured spatial acuity, defined as the angular distance between neighboring rhabdom centers, for two retinal regions: the acute zone and the medial periphery. The acute zone was defined as the region of highest photoreceptor density, located just lateral to the center of the ALE field of view. The medial periphery was defined as the portion of medial facing photoreceptors along the edge of the retina, located across from the acute zone and along the horizontal plane. To convert image pixel distances to angular distances, we measured the displacement, in pixels, of landmarks (e.g., irregularities or dark spots in the retinal mosaic) visible in pairs of consecutive retinal images that differed by a known angular increment (e.g., 10° or 15°). This measure was then used to calculate the number of pixels per degree for retinal images of that individual, with this process repeated for each individual in the study to account for minor differences in ophthalmoscope focusing between individuals and imaging sessions. Using this conversion, we then measured the angular distances between 10 neighboring photoreceptors per retinal region per individual. Differences between locations, developmental stages and/or timepoints were investigated using two-way, repeated-measures ANOVAs, with individual as a random factor, and time point and/or location nested within individual.

We measured the dimensions of the ALE field of view by quantifying the angular distance from retinal edge to retinal edge for two perpendicular axes: a vertical axis running through the center of the acute zone, and a horizontal axis which crossed the vertical axis at the acute zone center. Transects for these axes were created by manually assembling the appropriate series of images. The resulting dimensions corresponded to the actual horizontal and vertical planes of the spiders' field of view as closely as the precision of our goniometer mounting procedures allowed. Statistical analyses of field-of-view followed those described for spatial acuity above.

2.4. Histology

2.4.1. Histological preparation, sectioning, and imaging

Spiders were prepared for histological measurements by first euthanizing animals using gaseous CO_2 sublimated from dry ice. Whole cephalothoraxes were then fixed in 2.5% glutaraldehyde and stored in microcentrifuge tubes at ~4 °C prior to embedding. For larger spiders, fixed cephalothoraxes were further dissected by removing the chelicerae and perforating the posterior cephalothorax with minuten pins to improve infiltration during the embedding process. Following this initial preparation, tissue samples were washed three times in 0.1 M PBS (15 min per wash), stained with 2% osmium tetroxide for one hour, washed again in 0.1 M PBS (three 15-minute washes), and then dehydrated via an ethanol series (30%, 50%, 70%, 90%, 100%, 100%, 100%, 20 min each). Dehydrated specimens were washed three times (10 min per wash) in pure propylene oxide before incubating them in a series of increasing concentrations of a resin mixture (equal mixture by weight of EMbed 812 and Spurr's Resin) and propylene oxide (resin mixture:propylene oxide; 1:3, 1:1, 3:1, placed on a rotator overnight for each incubation). Specimens were then subjected to three hour-long washes in undiluted resin mixture before being positioned in resin-filled molds and baked overnight at 70 °C.

Resin-embedded cephalothoraxes were serially sectioned at 1–3 μm thicknesses using glass knives on a Reichert Ultracut E ultramicrotome (C. Reichert, Wien, Austria), and then stained with Toluidine blue. We sectioned individuals at a range of developmental stages, with individual preps sectioned in either the transverse plane (i.e. parallel to the horizontal plane of the cephalothorax) or the sagittal plane (i.e., perpendicular to both the horizontal plane and the anterior posterior axis). These sections were then imaged using a compound microscope (Zeiss microscope with Plan-NEOFLUAR 20x objective, Oberkochen, Germany) and a digital camera (Canon EOS Digital Rebel XTi, Tokyo, Japan).

2.4.2. Morphological measurements

We used the resulting section images to directly measure three properties of each ALE retina: rhabdom width, rhabdom length, and the distance between the centers of neighboring rhabdoms (interrhabdomal

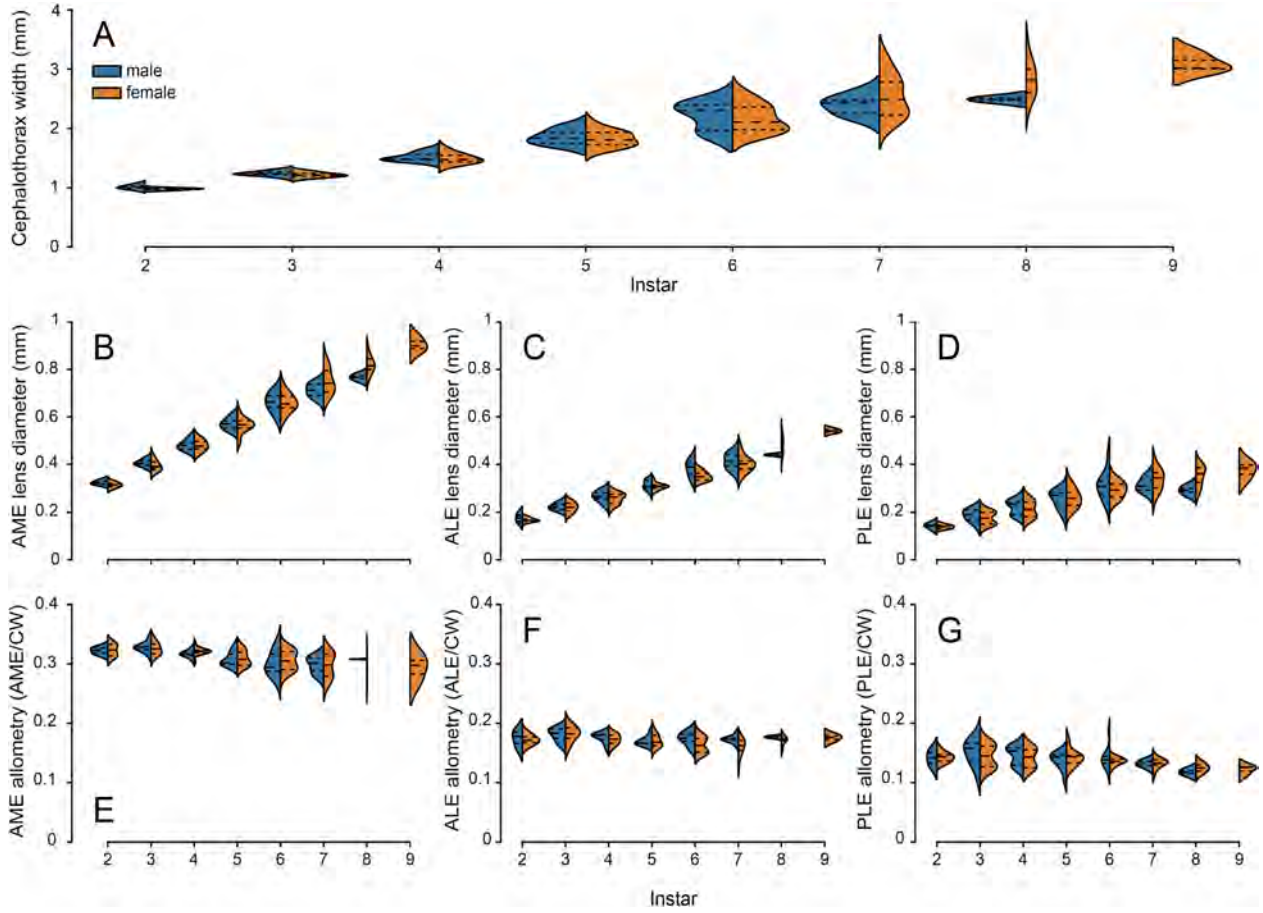

Fig. 3. Changes in body size and lens dimensions across developmental instars, including cephalothorax width (A), as well as the lens widths of the anterior medial eyes (AME, B), the anterior lateral eyes (ALE, C), and the posterior lateral eyes (PLE, D). Adult females have larger heads and eyes as a result of one-to-two additional instars of growth. All eyes exhibit negative allometry in lens growth across development (E–G), indicating that spiderlings start off with proportionally larger lenses in comparison to cephalothorax width.

distance, IRD). From each set of serial sections, we selected the section that traversed the retina closest to the center of the ALE acute zone. The acute zone was identified as the retinal region with the smallest IRDs and the longest rhabdoms. One such section was selected per individual; we then measured the widths and lengths of all rhabdoms in the section as well as all IRDs, running from retinal edge to retinal edge. For sagittal sections, this sectioning transect ran from dorsal to ventral retinal edges; in transverse sections, the transect ran from medial to lateral edges.

All three measurements were taken using ImageJ, with image dimensions calibrated using a stage micrometer. Rhabdom lengths were measured as the linear distance from the distal to proximal end of each rhabdom, with the latter defined as the point at the base of the retina where interrhabdomal screening pigments end and the rhabdom transitions to the cell body. Rhabdom width was measured as the width of the rhabdom at each photoreceptor's distal end. From these length and width measurements, we estimated the volume of each rhabdom using the equation for the volume of a cylinder ($\pi(width/2)^2 length$), based on prior observations that indicate these rhabdoms are approximately cylindrical (Blest, 1983; Eakin & Brandenburger, 1971). We then measured IRD as the distance between the centers of the distal ends of neighboring rhabdoms.

To compare retinal regions across developmental stages, we focused on three specific areas in these transects: the two peripheral regions at the edge of each transect, and the acute zone. The acute zone was designated as the area of the transect that had the smallest IRDs (indicating the highest photoreceptor density, and therefore the highest spatial acuity) and the longest rhabdoms. We found this joint criteria to more reliably identify the center of the acute zone than simply attending to IRD. For each individual, we averaged the measurements from a series of 10 adjacent photoreceptors per region.

In total, we sampled transects from 12 individuals for both transverse sections (H: $n = 5$ EJ: $n = 3$, LJ: $n = 2$, A: $n = 2$, one of each sex) and sagittal sections (H: $n = 3$, EJ: $n = 4$, LJ: $n = 3$, A: $n = 2$, one of each sex). Given the small sample sizes for each life stage, we focused our analysis on qualitative comparisons between life stages, rather than formal statistical comparisons.

2.5. Focal length assessment

To measure how the focal length of spider ALE and AME lenses change across development, we used a previously described, 'hanging-drop' method (Homann, 1924; Stowasser & Buschbeck, 2014). Briefly, individual lenses were dissected from freshly euthanized individuals and suspended from a coverslip with Ringer's solution (O'Shea & Adams, 1981). Using a microscope and camera, we then captured images of a target object as viewed through the mounted lens, with the target positioned in a series of focal points at 5 µm increments behind the lens. The target object was a square-wave grating (0.63 cycles/mm, USAF 1951 negative test target, Edmund Optics) illuminated with green light (peak wavelength 548 nm, half width 40 nm). This object was placed at a distance of 13 cm in front of the mounted lens. For each series, the best focused image was identified and the size of the target image measured using a customized MATLAB program that evaluates Michelson contrast (Stowasser & Buschbeck, 2014). The focal length of the lenses was calculated from the image size using the equation

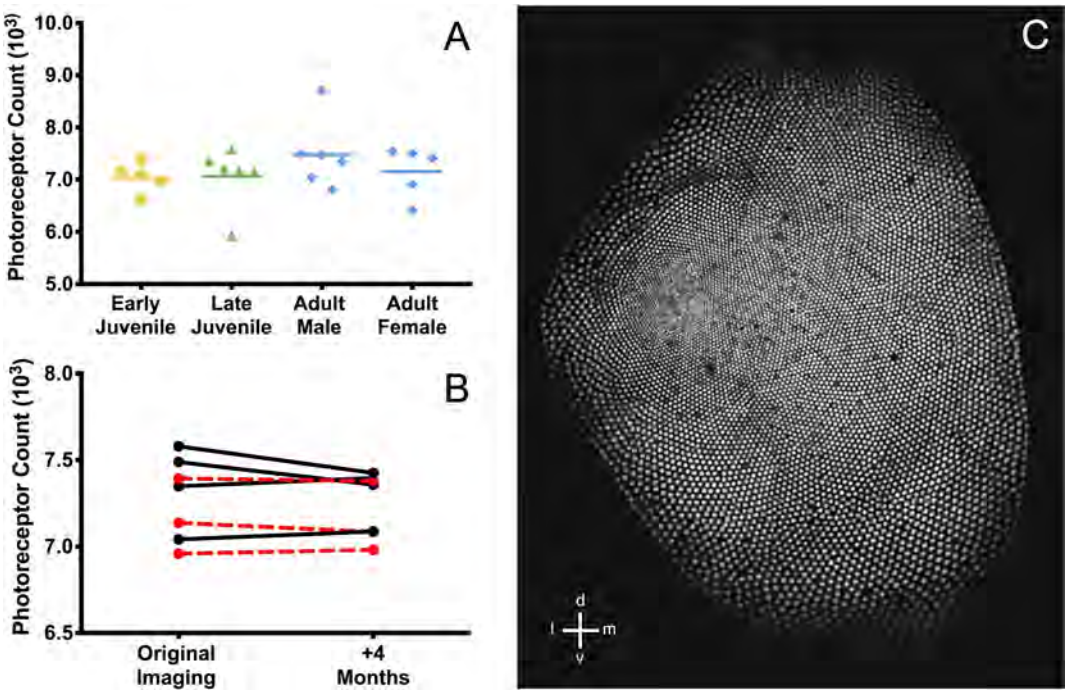

Fig. 4. Total photoreceptor count in ALE retinas remains the same across development when compared between individuals from different life stages (A), or within individuals across time (B). For re-imaged individuals (B), dashed red lines connect data points from individuals who molted to another developmental period (i.e., EJ to LJ or LJ to A) during the time between measurements, whereas black continuous lines represent individuals who did not. (C) Example of a composite ALE retinal map from ophthalmoscopic imaging, with orientation relative to body axes indicated in the bottom left as follows: dorsal (d), ventral (v), lateral (l), and medial (m). (For interpretation of the references to color in this figure legend, the reader is referred to the web version of this article.)

$$f = (y_i * o)/y_o$$

where y_i is the image size, y_o is the object size and o is the object distance.

In total, we measured the focal lengths of ALE and/or AME lenses for 19 individuals (H: $n = 1$, EJ: $n = 5$, LJ: $n = 4$, A: female $n = 6$, male $n = 4$). Hatchling data was excluded from formal statistical analysis, but is provided for comparison. Given that our groups from different developmental time points exhibited unequal variances and small sample sizes, we chose to analyze these focal length data with one-way Kruskal-Wallis tests. Post-hoc comparisons were conducted using Dunn's test.

3. Results

3.1. Developmental changes to external morphology

Over the course of development, *P. audax* increase dramatically in size (Fig. 3A), with males more than doubling their cephalothorax widths (CW means ± SE; 2nd instar: 1.01 ± 0.02 mm, adult: 2.49 ± 0.04 mm) and females tripling their CW (2nd instar: 0.98 ± 0.01 mm, adult: 3.09 ± 0.09 mm). Females become larger than males predominantly by extending their development for an additional 1–2 instars (Figs. 3A and A1), although analysis of sex-specific growth trajectories also indicates a slightly steeper slope to female CW growth (sex * instar interaction term: $F_{1,130.22} = 10.32$, $p = 0.002$). We also detected a significant difference between spiderling cohorts in their growth trajectories (cohort * instar interaction term: $F_{1,130.22} = 148.75$, $p < 0.001$), with spiders from our first cohort growing faster and achieving larger adult CW sizes (see Fig. A2).

Growth of the AME, ALE, and PLE lenses follow these patterns of overall cephalothorax growth (Fig. 3B–D). Male lenses grow to 2–3 times their 2nd instar diameter (AME, 2nd instar: 0.33 ± 0.01 mm, adult: 0.77 ± 0.01 mm; ALE, 2nd instar: 0.18 ± 0.01 mm, adult: 0.44 ± 0.01 mm; PLE, 2nd instar: 0.14 ± 0.01 mm, adult: 0.29 ± 0.02 mm). Female lenses grow to 3–4 times their 2nd instar diameter (AME, 2nd instar: 0.32 ± 0.01 mm, adult: 0.90 ± 0.02 mm; ALE, 2nd instar: 0.17 ± 0.01 mm, adult: 0.54 ± 0.01 mm; PLE, 2nd instar: 0.14 ± 0.01 mm, adult: 0.38 ± 0.02 mm). Lens diameters also exhibited a consistent effect of cohort on growth trajectories (cohort * instar interaction term; AME: $F_{1,130.17} = 7.07$, $p < 0.001$; ALE: $F_{1,133.19} = 7.16$, $p = 0.008$; PLE: $F_{1,132.75} = 12.54$, $p < 0.001$). However, only the AME showed evidence for sex-specific growth trajectories, with female AME exhibiting a slightly steeper growth slope (sex * instar interaction term; AME: $F_{1,130.17} = 6.05$, $p = 0.015$; ALE: $F_{1,133.19} = 0.51$, $p = 0.478$; PLE: $F_{1,132.75} = 0.42$, $p = 0.517$).

Although the lens diameters of all three eye pairs increased alongside overall cephalothorax width, their growth followed a pattern of negative allometry (Fig. 3E–G) with 2nd instar spiderlings exhibiting proportionately larger lenses compared to their subsequent adult morphology (slope estimates ± SE for relative lens diameter by instar; AME: $\beta = -0.013 \pm 0.0006$, $t_{132} = 20.10$, $p < 0.001$; ALE: $\beta = -0.006 \pm 0.0008$, $t_{151} = 7.18$, $p < 0.001$; PLE: $\beta = -0.008 \pm 0.0008$, $t_{134.83} = 9.61$, $p < 0.001$). These slopes were also more negative for the faster growing, and subsequently larger, first cohort of spiderlings (cohort * instar interaction term; AME: $F_{1,132} = 194.99$, $p < 0.001$; ALE: $F_{1,151} = 38.60$, $p < 0.001$; PLE: $F_{1,134.83} = 36.15$, $p < 0.001$). Males and females shared a common set of lens diameter allometric slope across development (sex * instar interaction term; AME: $F_{1,132} = 0.11$, $p = 0.741$; ALE: $F_{1,151} = 0.62$, $p = 0.432$; PLE: $F_{1,134.83} = 0.02$, $p = 0.902$).

3.2. ALE photoreceptor number

We find no evidence for a change in ALE photoreceptor numbers, either when compared across individuals from different developmental stages (Fig. 4A, $F_{3,18} = 0.83$, $p = 0.497$) or when compared within individuals across time points (Fig. 4B, t6 = 1.09, $p = 0.317$). Individuals of both sexes maintain slightly more than 7000 rhabdoms in their ALE

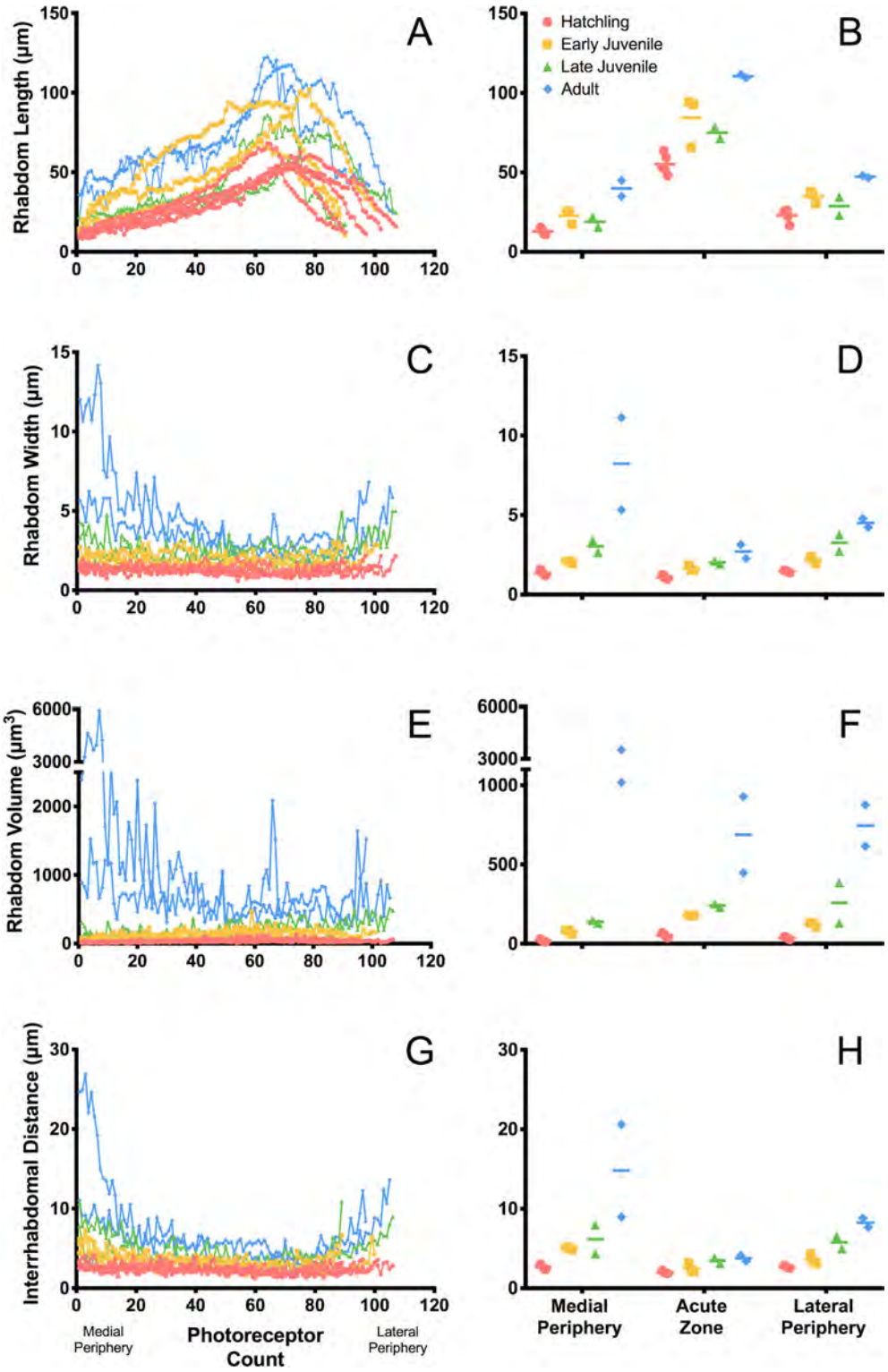

Fig. 5. Rhabdomal size and spacing measurements from the ALE retinas of individuals from different developmental stages, sectioned in the transverse plane. Raw measurements from individual sections are plotted for rhabdomal length (A), width (C), volume (E), and interrhabdomal distance (G), with the corresponding individual means (points) and group means (horizontal bars) for the indicated regions plotted to their right (B, D, F, and H respectively).

retinas from early development onward (photoreceptor count means ± SE; early juvenile: 7039.4 ± 129.7, late juvenile: 7063.7 ± 236.2, adult male: 7476.7 ± 269.6, adult female: 7153.2 ± 218.9). In addition, five out of seven re-imaged individuals exhibited a small decrease in total photoreceptor number, indicating that photoreceptors may be lost but are not gained after spiderling emergence from the egg sack.

3.3. Retinal histology

Retinal changes across development are clear and consistent for both sectioning planes (Fig. 5, Table 1). In the retinal periphery and central acute zone, rhabdoms increase in length (Figs. 5B and A3B) and width (Figs. 5D and A3D) over the course of development, resulting in dramatic increases in rhabdomal volume (i.e., sometimes by as much as

Table 1
Mean and standard error values from rhabdom measurements collected across life stages (H = hatchling, EJ = early juvenile, LJ = late juvenile, A = adult), for both transverse and sagittal sectioning planes.

Transverse:

	Length (μm)		Width (μm)		Volume (μm^3)		IRD (μm)	
	Mean	SE	Mean	SE	Mean	SE	Mean	SE
Medial Periphery								
H	12.92	0.89	1.34	0.07	18.89	3.38	2.65	0.12
EJ	22.70	2.67	2.06	0.06	76.59	8.09	4.99	0.09
LJ	18.89	3.32	3.03	0.39	138.42	9.26	6.17	1.83
A	39.94	5.05	8.23	2.90	2271.56	1253.44	14.80	5.81
Acute Zone								
H	55.19	2.81	1.09	0.05	52.98	5.97	2.00	0.07
EJ	84.30	9.31	1.63	0.11	178.55	0.68	2.47	0.34
LJ	74.97	3.60	2.01	0.10	241.33	11.15	3.49	0.34
A	110.48	1.14	2.70	0.44	687.73	240.57	3.76	0.37
Lateral Periphery								
H	23.08	1.77	1.45	0.03	37.03	3.67	2.65	0.06
EJ	34.81	2.31	2.17	0.13	122.83	8.68	3.58	0.37
LJ	28.78	5.74	3.26	0.52	258.34	127.61	5.77	0.76
A	47.32	0.73	4.51	0.28	745.95	130.27	8.23	0.58

Sagittal:

	Length (μm)		Width (μm)		Volume (μm^3)		IRD (μm)	
	Mean	SE	Mean	SE	Mean	SE	Mean	SE
Dorsal Periphery								
H	16.59	1.24	2.03	0.08	53.05	1.49	3.23	0.01
EJ	20.98	1.54	2.48	0.13	101.35	5.96	5.88	0.72
LJ	33.76	9.19	4.44	0.44	554.29	173.88	8.75	0.78
A	34.98	2.27	6.04	0.32	1024.85	169.68	12.32	3.79
Acute Zone								
H	48.67	0.73	1.05	0.06	43.21	4.90	1.77	0.21
EJ	88.89	2.87	1.32	0.14	126.51	25.27	2.37	0.29
LJ	87.07	5.69	2.37	0.15	386.55	35.37	3.68	0.51
A	109.95	9.31	2.61	0.09	610.29	102.07	3.29	0.15
Ventral Periphery								
H	11.57	1.14	1.73	0.18	28.96	9.87	2.55	0.09
EJ	20.17	1.86	2.34	0.21	87.41	14.15	4.69	0.27
LJ	21.38	1.67	4.16	0.35	296.15	47.25	9.18	0.64
A	30.88	0.77	5.13	0.48	649.45	120.35	7.91	2.27

an order of magnitude, Figs. 5F and A3F). In addition, interrhabdomal distances increased across development in all retinal regions (Figs. 5H and A3H). Thus, the overall pattern is one of increasing rhabdomal size and expanding rhabdomal spacing, resulting in an overall increase in retinal volume (e.g., Fig. 2B, C). It is also worth noting that rhabdom widths of hatchlings begin at or near the typical lower limit for optimal photoreceptor diameter (acute zone means ± SE: transverse: 1.09 ± 0.05 μm, sagittal: 1.05 ± 0.06 μm).

3.4. Spatial acuity and field of view

Our analysis of spatial acuity revealed consistent differences between the ALE acute zone and medial periphery (Fig. 6A; $F_{1,16} = 336.32$, $p < 0.001$), but no significant differences between developmental stages ($F_{2,16} = 0.17$, $p < 0.001$) and no significant effect of individual identity ($F_{16,16} = 1.10$, $p = 0.425$). These results were mirrored by patterns observed in re-measured individuals, with consistent differences between retinal regions (Fig. 6B; $F_{1,12} = 330.89$, $p < 0.001$) but no significant effect of time point ($F_{1,12} = 2.74 \times 10^{-5}$, $p = 0.996$) or individual identity ($F_{12,12} = 0.96$, $p = 0.530$). Interrhabbdomal angles within the acute zone were roughly half the size of those in the medial periphery (means ± SE; acute zone: 0.46 ± 0.01°, medial periphery, 1.05 ± 0.02°).

Similar patterns emerged from our analysis of ALE field-of-view. We found consistent differences in angular span between vertical and horizontal axes of the ALE field-of-view (Fig. 6C; $F_{1,16} = 842.58$, $p < 0.001$), but no significant differences between developmental stages ($F_{1,16} = 1.72$, $p = 0.211$). Individual identity was a significant predictor of variation in field-of-view ($F_{16,16} = 4.47$, $p = 0.002$). In general, the ALE field-of-view is larger in the vertical plane than the horizontal plane (means ± SE; vertical axis: 97.57 ± 1.93°, horizontal axis: 69.59 ± 0.74°).

Analysis of field-of-view results from re-imaged individuals were similar, but with some subtle differences. Re-measured individuals exhibited differences between axes (Fig. 6D; $F_{1,12} = 562.85$, $p < 0.001$) but not time points ($F_{1,12} = 0.41$, $p = 0.536$), and individual identity explained a significant amount of variation in field of view ($F_{12,12} = 8.58$, $p < 0.001$). However, the interaction between axis and time point was also significant ($F_{1,12} = 7.54$, $p = 0.018$), indicating that exact differences in axis dimensions depend on the time point they were measured (i.e., changes in axes between time points were not parallel). To investigate this interaction further, we performed paired *t*-tests on each axis independently. Consistent with the lack of a significant main effect of time point in our repeated-measures ANOVA analysis, our *t*-tests revealed no significant change in field-of-view between time points for the vertical ($t_6 = 1.09$, $p = 0.318$) or horizontal axis ($t_6 = 0.34$, $p = 0.748$). Thus, our overall analysis indicates that field-of-view does not change detectably over time, either when measured across development or over shorter periods of time.

3.5. Focal length

Focal lengths of both the ALE and AME increased across development (Fig. 6E). ALE focal lengths increased by more than twice (means ± SE, early juvenile: 0.20 ± 0.03 mm, late juvenile: 0.36 ± 0.01 mm, adult: 0.45 ± 0.01 mm), with adult focal lengths being significantly longer than those of early juveniles ($H = 12.71$, $p < 0.001$). Likewise, AME focal lengths more than doubled (means ± SE; early juvenile: 0.43 ± 0.03, late juvenile: 0.79 ± 0.03, adult: 1.04 ± 0.02), representing a significant difference between early juvenile and adult stages ($H = 14.37$, $p < 0.001$). Measurements of hatchling focal lengths fell largely within the range measured from early juveniles (Fig. 6E).

4. Discussion

Our examination of visual system changes across development provides a number of new insights into how jumping spiders develop their tiny eyes. First, we find that the lenses of all eye pairs develop following a pattern of negative ontogenetic allometry. Hatchling spiders emerge with larger lenses in proportion to their cephalothorax size than those of adults. This is a common strategy across vertebrate groups with single lens eyes (Augusteyn et al., 2016; Fernald, 1985; Harahush et al., 2009; Mitchell et al., 2013; Werner & Seifan, 2006), and arises as a means for ameliorating the impact of small size on light capture and other visual functions. Thus, jumping spiders can be added to the list of animal groups that employ this strategy during development.

In evaluating changes to the retinal photoreceptor mosaic of the ALE, our results indicate that jumping spiders do not add photoreceptors to these retinas post-embryonically. Instead, they hatch with their full adult complement of photoreceptors, a pattern hinted at by prior work on photoreceptor numbers in AME (Blest & Carter, 1987) but demonstrated conclusively here for the first time. Thus, jumping spider retinal development is similar to that observed in mammals and the larval eyes of diving beetles, both of which also halt photoreceptor differentiation following embryonic development (Kuhrt et al., 2012; Werner & Buschbeck, 2015). From a functional standpoint, this may

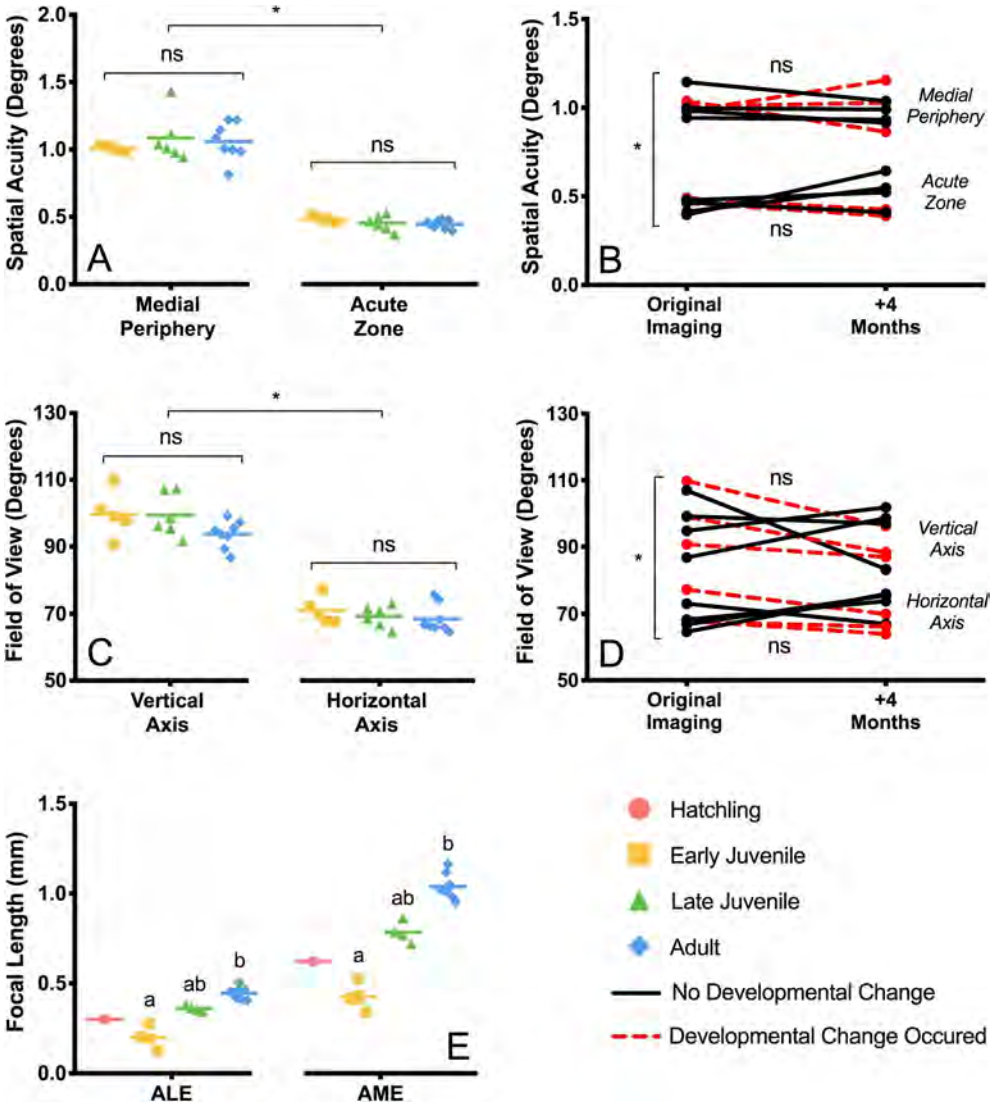

Fig. 6. Developmental changes in spatial acuity, field-of-view, and focal length. (A) Spatial acuity differed between retinal regions, but not between developmental stages across individuals (A) or time points measured within the same individuals (B). For the latter, data from individuals that molted to another developmental period are connected with dashed red lines, while those who didn't are connected by solid black lines. Similarly, the angular field-of-view differed between axis orientations, but not between developmental stages across individuals (C) or time points within individuals (D). Focal lengths increased across development for both ALE and AME (E). In (E), hatchling data are presented for comparison but not formally included in statistical analyses. Statistical differences are indicated as follows: (A–D) $^{*}p < 0.05$, ns: $p > 0.05$; (E) lowercase letters denote statistically distinct groups. (For interpretation of the references to color in this figure legend, the reader is referred to the web version of this article.)

appear suboptimal because it requires early instars to accommodate the large number of photoreceptors demanded by adult acuity needs within a substantially smaller cephalothorax volume. However, when combined with precise focal length increases and retinal growth, this can lead to maintaining a constant spatial acuity across development. In addition, this pattern is entirely consistent with predictions from insect developmental genetics, which would posit that photoreceptor differentiation should cease following the production of the lens (Charlton-Perkins & Cook, 2010; Kumar, 2012; Tsachaki & Sprecher, 2012).

The primary consequence of this developmental constraint is that early instars must find a way to fit a large number of photoreceptor cells (~7000 in *P. audax* ALE) into a small volume. How is this achieved? Our work indicates that jumping spiders do so by initiating post-embryonic development with short, narrow rhabdoms that subsequently grow in size. Intriguingly, ALE rhabdom diameters rarely fall below 1 μm, even in the earliest developmental stages. This is important because rhabdoms with smaller diameters would shift from operating as light guides with total internal reflection to waveguides (Warrant & McIntyre, 1993). Given that ALE photoreceptors are most sensitive to green light (λ_{max} = 536 nm, Yamashita & Tateda, 1976) and that the minimum rhabdom diameter to remain functional as a light guide would be approximately twice the wavelength of incident light, 1 μm sits right at this lower limit. This means that some of the narrowest rhabdoms are likely starting to adopt waveguide properties, with a portion of the energy from incident photons traveling outside the rhabdoms. As these cells tend to be surrounded by dense pigmentation (Blest, 1983), such light would be absorbed by screening pigment rather than crossing into neighboring units, preserving the high resolution of the retinal mosaic but at a cost in terms of sensitivity. Thus, there is unlikely to be any visual benefit to producing rhabdoms with smaller diameters, and perhaps even an increased sensitivity cost due to higher absorbance of light by screening pigments.

In *P. audax*, hatchlings appear to maximize the number of photoreceptors that are packed into their tiny retinas by starting with rhabdom diameters at this lower limit regardless of position in the retina. This finding hints at the intriguing possibility that rhabdom diameter minimums might constrain the number of ALE photoreceptors that fit into a hatchling cephalothorax, thereby indirectly limiting the number of photoreceptors available to adult ALE. If true, adult ALE resolution might be governed not so much by the visual requirements of adults, as by size limitations during early development, an idea that warrants testing in species with extremely small spiderlings and/or large changes in body size across development.

Following this hatchling phase, rhabdoms increase in diameter in all eye regions. However, different retinal regions engage in rhabdom growth in different ways. In the central acute zone, rhabdom diameter increases only modestly, whereas rhabdom length grows dramatically. In contrast, in the retinal periphery, rhabdom diameters increase more

than rhabdom lengths. The result is that ALE rhabdom volumes increase by more than an order of magnitude across all retinal regions. Given that light absorption by rhabdoms is directly related to rhadbomal volume (Land & Nilsson, 2012), these changes increase the overall sensitivity of the eye, but in distinct ways. By increasing their length more than their width, rhabdoms in the central acute zone are able to remain densely packed while still increasing their sensitivity, thereby supporting heightened contrast sensitivity while retaining high spatial acuity. Rhabdoms in the periphery, on the other hand, increase their width more than their length, ultimately resulting in much larger volumes (i.e., because the volume of a cylinder increases only linearly with length, but at the square of its radius) and therefore much higher sensitivity. However, given their larger diameters, these rhabdoms must be spaced farther apart, leading to reduced spatial acuity in the periphery compared to the acute zone. These patterns of growth appear to support regionally distinct visual functions: high spatial acuity in the central acute zone and enhanced sensitivity in the retinal periphery (which could support improved motion detection, Zurek & Nelson, 2012a, 2012b).

While growth of the rhabdoms increases the sensitivity of the ALE photoreceptors as spiderlings develop, it is clear that the eyes of early juvenile stages have substantially lower sensitivity. But how much lower is the visual sensitivity of hatchlings compared to their adult counterparts? One way to assess this is to calculate sensitivity, S, with the following equation (Land, 1981):

$$S = \left(\frac{\pi}{4}\right)^2 \cdot \left(\frac{A}{f}\right)^2 \cdot d^2 \cdot (1 - e^{-kx}) \quad (1)$$

where A is the aperture (estimated here as 70% of lens diameter measurements), f is the focal length, d is the width of the rhabdoms, k is the absorption coefficient (taken from Barnes and Goldsmith (1977)) and x is the length of the rhabdoms. By using measurements from our study, we estimate that S values for hatchlings are between 0.09 (acute zone) and 0.07 (lateral periphery). Adult eyes exhibit markedly increased sensitivity, with S estimates from the acute zone of 1.1 (~12 times more sensitive than hatchlings) and the lateral periphery of 1.6 (~23 times more sensitive). These values suggest that the ALE of juvenile spiders are substantially more light limited than those of adults, and likely only achieve full visual acuity under direct sunlight. As their eyes and retinas grow, these sensitivity values improve, with higher sensitivities achieved more rapidly in the periphery due to this region's more pronounced increases in rhabdom diameter.

Although a number of morphological properties change dramatically across development, our results indicate that two key metrics of visual function remain constant: spatial acuity and field of view. Spatial acuity differs across the ALE visual field, consistent with differences in rhabdomal packing of the photoreceptor mosaic. However, early juveniles emerge from the egg sac with spatial acuities equivalent to those observed in adults. Likewise, ALE field of view appears to remain the same across development. This is a rather striking result given that so many parts of the eye are changing together. However, it implies strong selection for the retention of a consistent view of the world across development, achieved through careful coordination of disparate eye components and associated developmental pathways.

Three critical eye properties must change precisely to underwrite the observed constancy of spatial acuity and field of view: focal lengths (1) must increase in concert with both the changing position of the retina (2) and the expanding dimensions of the retinal mosaic (3) following to photoreceptor growth. Our results indicate that focal length increases gradually across developmental instars in both the ALE and AME, thereby accommodating the increasing distance between the lens and the growing retina. In addition, the increase in lens diameter occurs in near perfect concert, resulting in maintenance of the aspect ratio of the eye, a property characterized by the F-number (F; Land & Nilsson, 2012; Warrant & McIntyre, 1993) via following the equation

$$F = f/A \quad (2)$$

where f is the focal length, and A is the aperture. For hatchling ALE, we estimate F as approximately 1.59 ($f \approx 200\,\mu m$, $A \approx 126\,\mu m$); in adults, our estimate of F is nearly identical ($F = 1.45$, $f \approx 446\,\mu m$, $A \approx 308\,\mu m$). For the AME, our estimate of F in hatchlings is 1.84 ($f \approx 425\,\mu m$, $A \approx 231\,\mu m$), and 1.93 in adults, ($f \approx 1039\,\mu m$, $A \approx 539\,\mu m$). These low F values suggest that both the ALE and AME eyes are well equipped for efficient light capture throughout development (Warrant & McIntyre, 1993). However, such low F-numbers, typical of arthropod simple lens eyes, can result in issues with rhabdom light guide performance due to steeper angles of incidence for incoming light rays (Warrant & McIntyre, 1993). In *P. audax*, this problem is likely ameliorated by the extensive screening pigmentation surrounding their ALE rhabdoms. However, the AME rhabdoms are not individually surrounded by screening pigments, which may help to explain why these rhabdoms improve their light guiding performance by enhancing the refractive index difference between the rhabdomeres and their cytoplasmic surround (Blest & Carter, 1988).

In summary, we find that the eyes of hatchling jumping spiders exhibit many of the properties of their subsequent adult visual systems, including a full photoreceptor complement, high visual acuity, an equivalent field of view, and low F numbers. This is remarkable given the dramatic changes in size that elements of these eyes undergo across development, and suggests strong selection for tight developmental coordination between distinct visual system elements. In light of these results, it is perhaps not surprising that spiderling behavioral repertoires exhibit many of the same complex behaviors found in adults.

However, spiderling visual systems do not fully reproduce adult visual competencies. The clearest sacrifice made by juvenile eyes is dramatically lower light sensitivity, at least at the level of the photoreceptor array. This arises due to space constraints on the developing retina, paired with the apparent developmental constraint that photoreceptor differentiation is restricted to the embryonic stage and/or the need for maintaining acuity across life stages. The result, that hatchling AL eyes are predicted to be as much as 12–23 times less sensitive than their adult counterparts, means that juvenile spiders may struggle with visually guided tasks in all but the brightest light environments. Many jumping spiders, *P. audax* included, live in open habitats like old-fields and grasslands. However, even in these environments, changes to meteorological conditions or time of day may restrict the visually guided activities of juveniles. How might these animals cope, assuming that they don't just restrict activity? Two neurophysiological solutions are possible: temporal summation and spatial summation. It is also possible that these animals use a combination of both solutions across the eye, or different solutions in a retinal region-specific way (i.e., temporal summation in one portion of their field of view, and spatial summation in another portion, as has been recently described in *Drosophila*, Currea, Smith, & Theobald, 2018). Alternatively, juveniles may compensate by hunting only under favorable light conditions. Investigating whether early life stages of *P. audax* engage in summation of either type, or compensate behaviorally, would be extremely useful. Such behavioral and neuroethological questions would be exciting next steps as we better understand how small animals optimize the functional utility of their developing eyes.

Acknowledgments

We thank Annette Stowasser for her crucial support in hanging drop procedures, ophthalmoscope measurements and comments on earlier versions of the manuscript, Tom Harper for his mentorship during histological sectioning, Sebastian Echeverri and Riley Timbs for assistance in coding for image analysis, and Martin Turcotte for generously providing a workspace to JTG and PB during the late stages of the project. Special thanks to the past members of the Morehouse Lab Spider Team for assistance with animal care: Taha Ahmed, Sinjon

Bartel, Corey Forman, Abby Jarrett, Ciara Kernan, Julia Kerstetter, Margaret Mass, Nick Russo, Emma Schanzenbach, Stanton Young, and Zachary Zimmer. This research was supported by funding to JTG from the University of Pittsburgh's Department of Biological Sciences, Honors College, and Biomedical Masters Program and funding to NIM from the University of Pittsburgh and the University of Cincinnati. Part of this research was supported by the National Science Foundation (grant IOS-1456757 to EKB). We also thank Michael Land for his pioneering work on jumping spider vision, which inspired both the questions our work asked and the methods we used to answer them.

Data

All data from this research can be found archived at Mendeley Data (doi: http://dx.doi.org/10.17632/v7mc8yzvd2.1).

Supplementary data

Supplementary data associated with this article can be found, in the online version, at https://doi.org/10.1016/j.visres.2019.04.006.

References

Abramoff, M. D., Magalhaes, P. J., & Ram, S. J. (2004). Image processing with ImageJ. *Biophotonics International, 11*(7), 36–42.
Augusteyn, R. C. (2014). Growth of the eye lens: II. Allometric studies. *Molecular Vision, 20*, 427–440.
Augusteyn, R. C., Maceo Heilman, B., Ho, A., & Parel, J.-M. (2016). Nonhuman primate ocular biometry. *Investigative Ophthalmology & Visual Science, 57*(1), 105–114.
Barnes, S. N., & Goldsmith, T. H. (1977). Dark-adaptation, sensitivity, and rhodopsin levels in eye of lobster, Homarus momarus. *Journal of Comparative Physiology, 120*, 143–159.
Bartos, M. (2008). Alternative predatory tactics in a juvenile hunting spider. *Journal of Arachnology, 36*(2), 300–305.
Bartos, M., & Szczepko, K. (2012). Development of prey-specific predatory behavior in a jumping spider (Araneae: Salticidae). *Journal of Arachnology, 40*(2), 228–233.
Bates, D., Maechler, M., Bolker, B., & Walker, S. (2015). Fitting linear mixed-effects models using lme4. *Journal of Statistical Software, 67*(1), 1–48.
Berry, D. S., & McArthur, L. Z. (1986). Perceiving character in faces: The impact of age-related craniofacial changes on social perception. *Psychological Bulletin, 100*(1), 3–18.
Blest, A. D. (1983). Ultrastructure of secondary retinae of primitive and advanced jumping spiders (Araneae, Salticidae). *Zoomorphology, 102*, 125–141.
Blest, A. D., & Carter, M. (1987). Morphogenesis of a tiered principal retina and the evolution of jumping spiders. *Nature, 328*, 152–155.
Blest, A. D. (1988). Post-embryonic development of the principal retina of a jumping spider I. The establishment of receptor tiering by conformational changes. *Philosophical Transactions of the Royal Society B: Biological Sciences, 320*(1201), 489–504.
Blest, A. D., & Carter, M. (1988). Post-embryonic development of the principal retina of a jumping spider II. The acquisition and reorganization of rhabdomeres and growth of the glial matrix. *Philosophical Transactions of the Royal Society B: Biological Sciences, 320*(1201), 505–515.
Charlton-Perkins, M., & Cook, T. A. (2010). Building a fly eye: Terminal differentiation events of the retina, corneal lens, and pigmented epithelia. *Invertebrate and Vertebrate Eye Development, 93*, 129–173.
Clark, D. L., & Uetz, G. W. (1993). Signal efficacy and the evolution of male dimorphism in the jumping spider, Maevia inclemens. *Proceedings of the National Academy of Sciences of the United States of America, 90*(24), 11954–11957.
Cross, F. R., & Jackson, R. R. (2017). Representation of different exact numbers of prey by a spider-eating predator. *Interface Focus, 7*, 20160035.
Currea, J. P., Smith, J. L., & Theobald, J. C. (2018). Small fruit flies sacrifice temporal acuity to maintain contrast sensitivity. *Vision Research, 149*, 1–8.
Eakin, R. M., & Brandenburger, J. L. (1971). Fine structure of the eyes of jumping spiders. *Journal of Ultrastructure Research, 37*, 618–663.
Elias, D. O., Maddison, W. P., Peckmezian, C., Girard, M. B., & Mason, A. C. (2012). Orchestrating the score: Complex multimodal courtship in the *Habronattus coecatus* group of Habronattus jumping spiders (Araneae: Salticidae). *Biological Journal of the Linnean Society, 105*(3), 522–547.
Fenk, L. M., Heidlmayr, K., Lindner, P., & Schmid, A. (2010). Pupil size in spider eyes is linked to post-ecdysal lens growth. *PLoS One, 5*(12), e15838.
Fernald, R. D. (1985). Growth of the teleost eye: Novel solutions to complex constraints. *Environmental Biology of Fishes, 13*(2), 113–123.
Flitcroft, D. I. (2014). Emmetropisation and the aetiology of refractive errors. *Eye, 28*(2), 169–179.
Friedrich, M. (2006). Continuity versus split and reconstitution: Exploring the molecular developmental corollaries of insect eye primordium evolution. *Developmental Biology, 299*, 310–329.
Girard, M. B., Kasumovic, M. M., & Elias, D. O. (2011). Multi-modal courtship in the peacock spider, Maratus volans (O.P.-Cambridge, 1874). *PLoS One, 6*(9), e25390.
Groeger, G., Cotton, P. A., & Williamson, R. (2005). Ontogenetic changes in thevisual acuity of Sepia officinalis measured using the optomotor response. *Canadian Journal of Zoology, 83*, 274–279.
Harland, D. P., Li, D., & Jackson, R. R. (2012). How jumping spiders see the world. In O. F. Lazareva, T. Shimizu, & E. A. Wasserman (Eds.). *How animals see the world: Comparative behavior, biology, and evolution of vision* (pp. 133–163). Press: New York, Oxford University.
Harahush, B. K., Hart, N. S., Green, K., & Collin, S. P. (2009). Retinal neurogenesis and ontogenetic changes in the visual system of the brown banded bamboo shark, Chiloscyllium punctatum (Hemiscyllidae, Elasmobranchii). *Journal of Comparative Neurology, 513*(1), 83–97.
Hairston, N. G., Li, K. T., & Easter, S. S. (1982). Fish vision and the detection of planktonic prey. *Science, 218*, 1240–1242.
Hinde, R. A., & Barden, L. A. (1985). The evolution of the teddy bear. *Animal Behaviour, 33*, 1371–1373.
Hoefler, C. D., & Jakob, E. M. (2006). Jumping spiders in space: Movement patterns, nest site fidelity and the use of beacons. *Animal Behaviour, 71*(1), 109–116.
Hofstetter, H. W. (1969). Emmetropization—Biological process or mathematical artifact? *American Academy of Optometry American Academy of Optometry, 46*, 447–450.
Homann, H. (1924). Zum Problem der Ocellenfunktion bei den Insekten. *Zeitschrift für vergleichende Physiologie, 1*, 541–578.
Homann, H. (1928). Beiträge zur Physiologie der Spinnenaugen. *Journal of Comparative Physiology A: Neuroethology, Sensory, Neural, and Behavioral Physiology, 7*(2), 201–268.
Howland, H. C., Merola, S., & Basarab, J. R. (2004). The allometry and scaling of the size of vertebrate eyes. *Vision Research, 44*(17), 2043–2065.
Howlett, M. H., & McFadden, S. A. (2007). Emmetropization and schematic eye models in developing pigmented guinea pigs. *Vision Research, 47*(9), 1178–1190.
Jackson, R. R., & Wilcox, R. S. (1990). Aggressive mimicry, prey-specific predatory behaviour and predator-recognition in the predator-prey interactions of Portia fimbriata and Euryattus sp., jumping spiders from Queensland. *Behavioral Ecology and Sociobiology, 26*, 111–119.
Jackson, R. R., & Pollard, S. (1996). Predatory behavior of jumping spiders. *Annual Review of Entomology, 41*, 287–308.
Jackson, R. R., Nelson, X. J., & Sune, G. O. (2005). A spider that feeds indirectly on vertebrate blood by choosing female mosquitoes as prey. *Proceedings of the National Academy of Sciences of the United States of America, 102*, 15155–15160.
Kuhrt, H., Gryga, M., Wolburg, H., Joffe, B., Grosche, J., Reichenbach, A., & Noori, H. R. (2012). Postnatal mammalian retinal development: Quantitative data and general rules. *Progress in Retinal and Eye Research, 31*(6), 605–621.
Kumar, J. P. (2012). Building an ommatidium one cell at a time. *Developmental Dynamics, 241*, 136–149.
Labhart, T., & Nilsson, D. E. (1995). The dorsal eye of the dragonfly sympetrum: Specializations for prey detection against the blue sky. *Journal of Comparative Physiology A: Neuroethology, Sensory, Neural, and Behavioral Physiology, 176*(4), 437–453.
Land, M. F. (1969a). Movements of the retinae of jumping spiders in response to visual stimuli. *The Journal of Experimental Biology, 51*, 471–493.
Land, M. F. (1969b). Structure of the retinae of the principal eyes of jumping spiders (Salticidae: Dendryphanatidae) in relation to visual optics. *The Journal of Experimental Biology, 51*, 443–470.
Land, M. F. (1981). Optics and vision in invertebrates. In H. Autrum (Vol. Ed.), *Comparative physiology and evolution of vision in invertebrates, Handbook of sensory physiology VII/6B: vol. VII/6B*, (pp. 471–592). Berlin/Heidelberg/New York: Springer.
Land, M. F. (1985a). Fields of view of the eyes of primitive jumping spiders. *The Journal of Experimental Biology, 119*, 381–384.
Land, M. F. (1985b). The morphology and optics of spider eyes. In F. G. Barth (Ed.). *Neurobiology of arachnids* (pp. 53–78). Berlin: Springer.
Land, M. F., & Nilsson, D. E. (2012). *Animal Eyes*. OUP Oxford.
Lim, M. L. M., & Li, D. (2004). Courtship and male-male agonistic behaviour of Cosmophasis umbratica Simon, an ornate jumping spider (Araneae: Salticidae) from Singapore. *Raffles Bulletin of Zoology, 52*(2), 435–448.
Lim, M. L. M., Li, J. J., & Li, D. (2008). Effect of UV-reflecting markings on female mate-choice decisions in Cosmophasis umbratica, a jumping spider from Singapore. *Behavioral Ecology, 19*(1), 61–66.
Liu, Z. Y., & Friedrich, M. (2004). The *Tribolium* homologue of glass and the evolution of insect larval eyes. *Developmental Biology, 269*, 36–54.
Mark, H. H. (1972). Emmetropization: Physical aspects of a statistical phenomenon. *Annals of Ophthalmology, 4*, 393–401.
McGinley, R. H., Mendez, V., & Taylor, P. W. (2015). Natural history and display behaviour of *Servaea incana*, a common and widespread Australian jumping spider (Araneae: Salticidae). *Australian Journal of Zoology, 63*, 300–319.
Miller, T. J., Crowder, L. B., & Rice, J. A. (1993). Ontogenetic changes in behavioural and histological measures of visual acuity in three species of fish. *Environmental Biology of Fishes, 37*, 1–8.
Mitchell, G., Roberts, D. G., van Sittert, S. J., & Skinner, J. D. (2013). Orbit orientation and eye morphometrics in giraffes (Giraffa camelopardalis). *African Zoology, 48*(2), 333–339.
Morehouse, N. I., Buschbeck, E. K., Zurek, D. B., Steck, M., & Porter, M. L. (2017). Molecular evolution of spider vision: New opportunities, familiar players. *Biological Bulletin, 233*, 21–38.
Morris, P. H., Reddy, V., & Bunting, R. C. (1995). The survival of the cutest: Who's responsible for the evolution of the teddy bear? *Animal Behaviour, 50*, 1697–1700.
Nagata, T., Koyanagi, M., Tsukamoto, H., Saeki, S., Isono, K., Shichida, Y., ... Terakita, A. (2012). Depth perception from image defocus in a jumping spider. *Science, 335*, 469–471.
Nelson, X. J., Jackson, R. R., & Sune, G. O. (2005). Use of Anopheles-specific prey-capture

behavior by the small juveniles of Evarcha culicivora, a mosquito-eating jumping spider. *Journal of Arachnology, 33*, 541–548.
Nelson, X. J., & Jackson, R. R. (2007). Complex display behaviour during the intraspecific interactions of myrmecomorphic jumping spiders (Araneae, Salticidae). *Journal of Natural History, 41*(25–28), 1659–1678.
Nelson, X. J., & Jackson, R. R. (2011). Flexibility in the foraging strategies of spiders. In M. E. Herberstein (Ed.). *Spider behaviour. Flexibility and versatility* (pp. 31–56). Cambridge, UK: Cambridge University Press.
Nelson, X. J., & Jackson, R. R. (2012a). The discerning predator: Decision rules underlying prey classification by a mosquito-eating jumping spider. *The Journal of Experimental Biology, 215*, 2255–2261.
Nelson, X. J., & Jackson, R. R. (2012b). The role of numerical competence in a specialized predatory strategy of an araneophagic spider. *Animal Cognition, 15*(4), 699–710.
O'Shea, M., & Adams, M. E. (1981). Pentapeptide (proctolin) associated with an identified neuron. *Science, 213*, 567–569.
Peckmezian, T., & Taylor, P. W. (2015). A virtual reality paradigm for the study of visually mediated behaviour and cognition in spiders. *Animal Behaviour, 107*, 87–95.
R Core Team (2018). *R: A language and environment for statistical computing.* URL:Vienna, Austria: R Foundation for Statistical Computing. https://www.R-project.org/.
Rutowski, R. L., Gislen, L., & Warrant, E. J. (2009). Visual acuity and sensitivity increase allometrically with body size in butterflies. *Arthropod Structure & Development, 38*(2), 91–100.
Schmucker, C., & Schaeffel, F. (2004). A paraxial schematic eye model for the growing C57BL/6 mouse. *Vision Research, 44*, 1857–1867.
Schomburg, C., Turetzek, N., Schacht, M. I., Schneider, J., Kirfel, P., Prpic, N. M., & Posnien, N. (2015). Molecular characterization and embryonic origin of the eyes in the common house spider Parasteatoda tepidariorum. *Evodevo, 6*, 15.
Stahl, A. L., Baucom, R. S., Cook, T. A., & Buschbeck, E. K. (2017). A complex lens for a complex eye. *Integrative and Comparative Biology, 57*, 1071–1081.
Stowasser, A., & Buschbeck, E. K. (2014). Multitasking in an eye: How the unusual organization of the principal larval eyes of Thermonectus marmoratus allows for far and near vision and might aid in depth perception. *Journal of Experimental Biology, 217*, 2509–2516.
Stowasser, A., Owens, M., & Buschbeck, E. K. (2017). Giving invertebrates an eye exam: An ophthalmoscope that utilizes the autofluorescence of photoreceptors. *Journal of Experimental Biology, 220*(22), 4095–4100.
Tarsitano, M. S., & Andrew, R. (1999). Scanning and route selection in the jumping spider Portia labiata. *Animal Behaviour, 58*, 255–265.
Tarsitano, M. S., & Jackson, R. R. (1997). Araneophagic jumping spiders discriminate between detour routes that do and do not lead to prey. *Animal Behaviour, 53*, 257–266.
Taylor, B. B., & Peck, W. B. (1975). A comparison of northern and southern forms of *Phidippus audax* (Hentz) (Araneida, Salticidae). *Journal of Arachnology, 2*, 89–99.
Taylor, L. A., & McGraw, K. J. (2013). Male ornamental coloration improves courtship success in a jumping spider, but only in the sun. *Behavioral Ecology, 24*(4), 955–967.
Taylor, L. A., Maier, E. B., Byrne, K. J., Amin, Z., & Morehouse, N. I. (2014). Colour use by tiny predators: Jumping spiders show colour biases during foraging. *Animal Behaviour, 90*, 149–157.
Taylor, L. A., Amin, Z., Maier, E. B., Byrne, K. J., & Morehouse, N. I. (2016). Flexible color-learning in an invertebrate predator: Habronattus jumping spiders can learn to prefer or avoid the color red when foraging. *Behavioral Ecology, 27*(2), 520–529.
Tsachaki, M., & Sprecher, S. G. (2012). Genetic and developmental mechanisms underlying the formation of the *Drosophila* compound eye. *Developmental Dynamics, 241*, 40–56.
Waller, B. M., Peirce, K., Caeiro, C. C., Scheider, L., Burrows, A. M., McCune, S., & Kaminski, J. (2013). Paedomorphic facial expressions give dogs a selective advantage. *PLoS One, 8*(12), e82686.
Wallman, J., & Winawer, J. (2004). Homeostasis of eye growth and the question of myopia. *Neuron, 43*(4), 447–468.
Warrant, E., & McIntyre, P. D. (1993). Arthropod eye design and the physical limits to spatial resolving power. *Progress in Neurobiology, 40*, 413–461.
Werner, S., & Buschbeck, E. K. (2015). Rapid and step-wise eye growth in molting diving beetle larvae. *Journal of Comparative Physiology A: Neuroethology, Sensory, Neural, and Behavioral Physiology, 201*, 1091–1102.
Werner, Y. L., & Seifan, T. (2006). Eye size in geckos: Asymmetry, allometry, sexual dimorphism, and behavioral correlates. *Journal of Morphology, 267*(12), 1486–1500.
Williams, D. S., & McIntyre, P. (1980). The principal eyes of a jumping spider have a telephoto component. *Nature, 288*, 578–580.
Yamashita, S., & Tateda, H. (1976). Spectral sensitivities of jumping spider eyes. *Journal of Comparative Physiology A: Neuroethology, Sensory, Neural, and Behavioral Physiology, 105*(1), 29–41.
Zurek, D. B., & Nelson, X. J. (2012a). Saccadic tracking of targets mediated by the anterior-lateral eyes of jumping spiders. *Journal of Comparative Physiology A: Neuroethology, Sensory, Neural, and Behavioral Physiology, 198*(6), 411–417.
Zurek, D. B., & Nelson, X. J. (2012b). Hyperacute motion detection by the lateral eyes of jumping spiders. *Vision Research, 66*, 26–30.
Zurek, D. B., Cronin, T. W., Taylor, L. A., Byrne, K., Sullivan, M. G. L., & Morehouse, N. I. (2015). Spectral filtering enables trichromatic vision in colorful jumping spiders. *Current Biology, 25*(10), R403–R404.

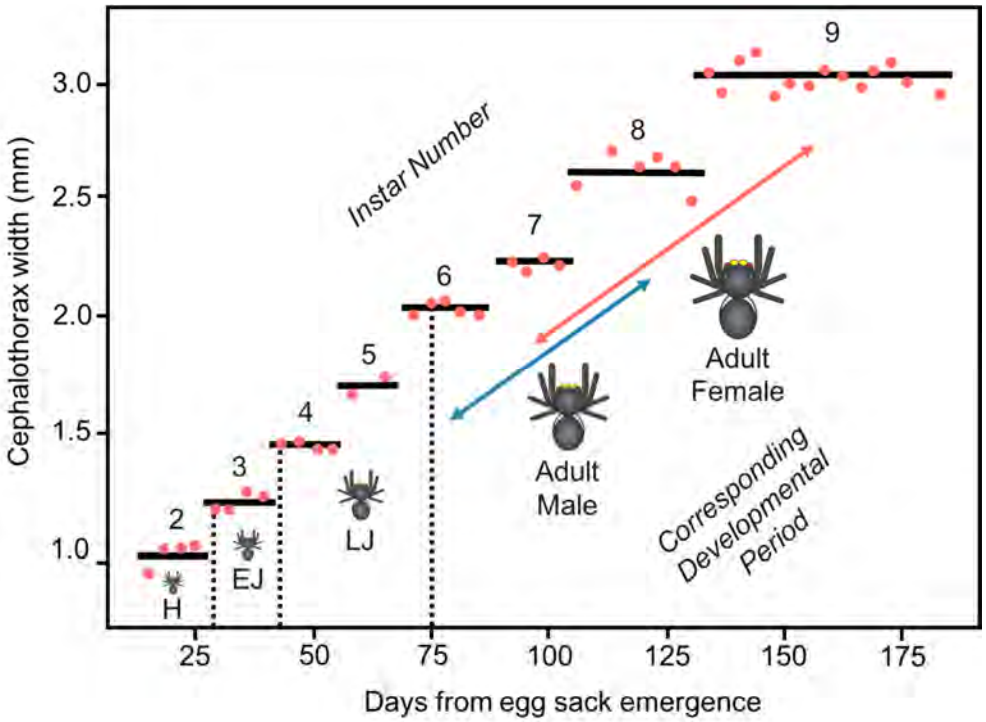

Figure A.1. Growth pattern of jumping spiders across development, displaying instar number and corresponding designation of developmental period (H = hatchling, EJ = early juvenile, LJ = late juvenile). Male are fully matured in 6-8 instars while females take 7-9 instars to reach maturity.

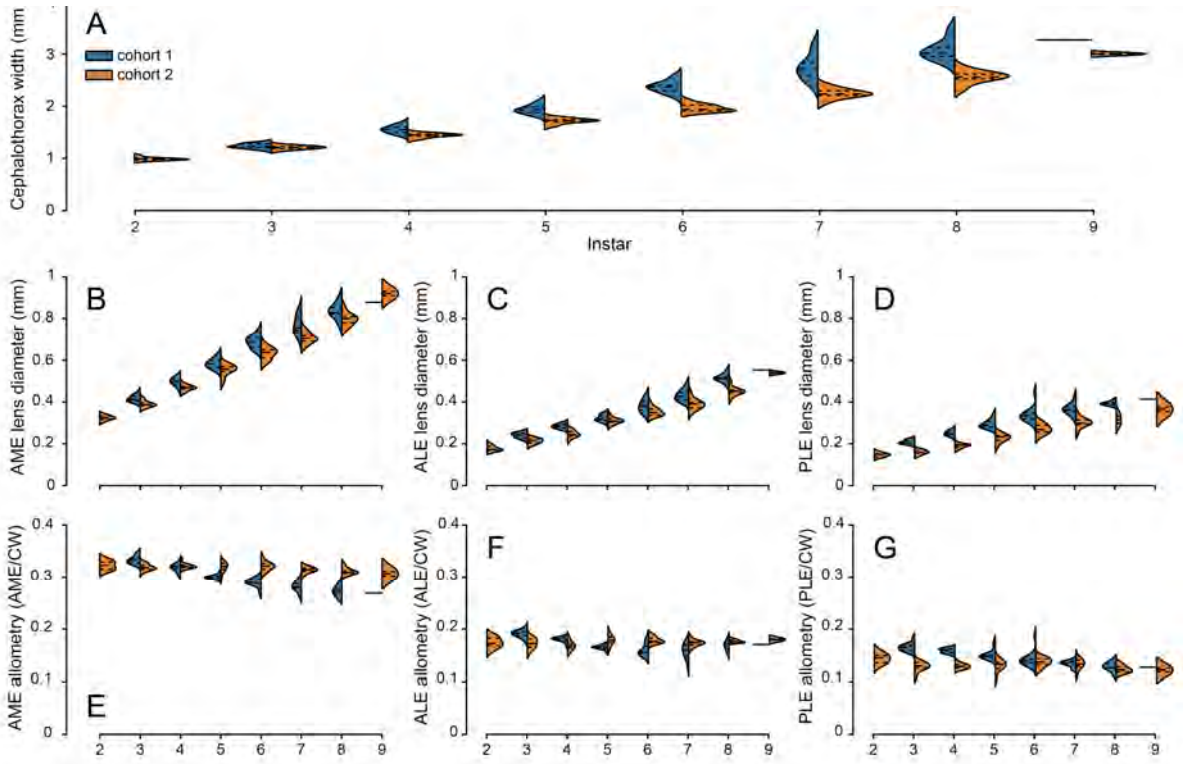

Figure A.2. Changes in body size and lens dimensions across developmental instars split by cohort, including cephalothorax width (A), as well as the lens widths of the anterior medial eyes (AME, B), the anterior lateral eyes (ALE, C), and the posterior lateral eyes (PLE, D). Cohort 1 represents individuals reared in 2015, whereas cohort 2 were reared in 2016. Individuals in cohort 1 grew faster and to larger adult sizes. All eyes exhibit negative allometry in lens growth across development (E-G), although negative allometry was more pronounced for cohort 1 than for cohort 2.

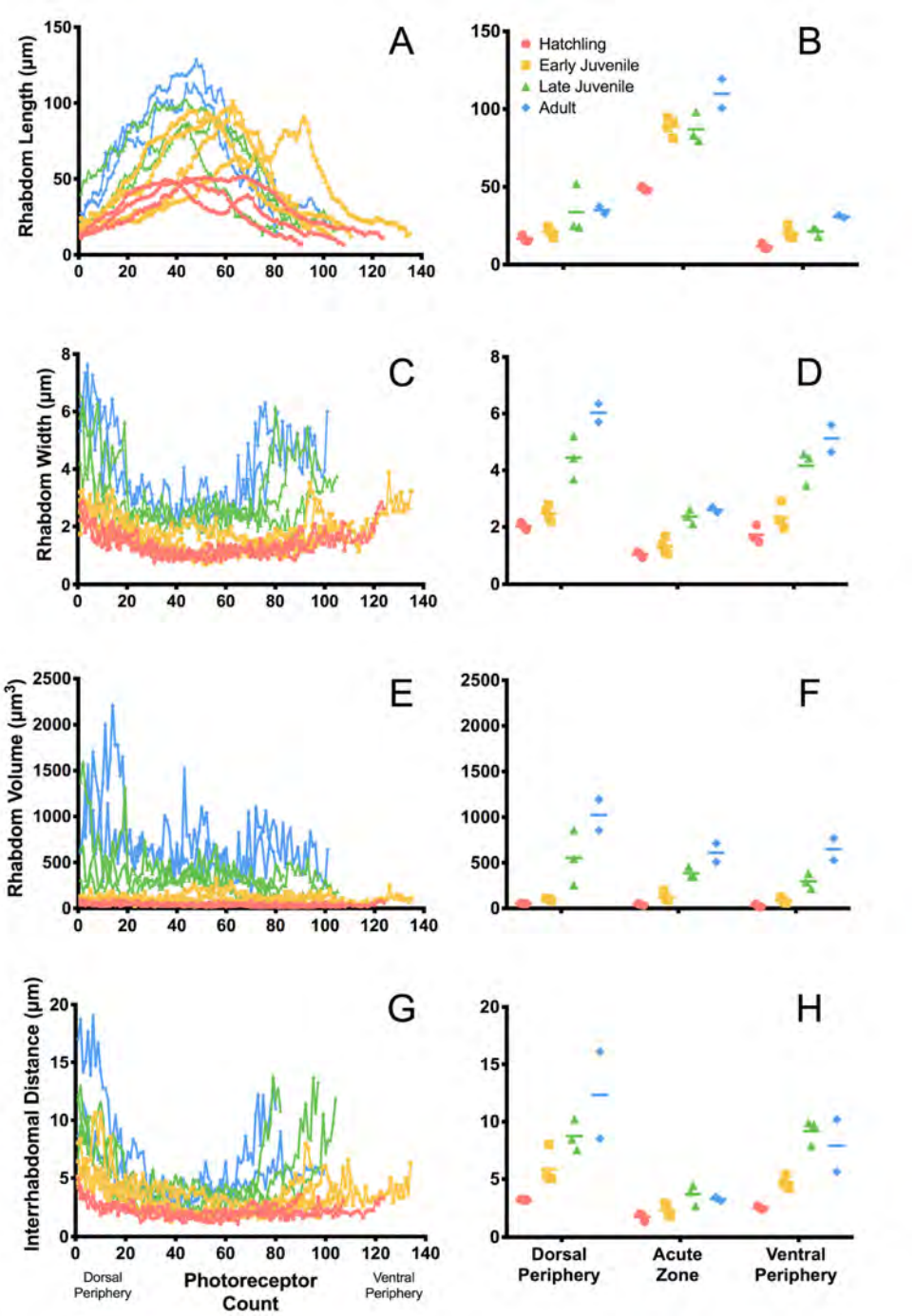

Figure A.3. Rhabdomal size and spacing measurements from the ALE retinas of individuals from different developmental stages, sectioned in the sagittal plane. Raw measurements from individual sections are plotted for rhabdomal length (A), width (C), volume (E), and interrhabdomal distance (G), with the corresponding individual means (points) and group means (horizontal bars) for the indicated regions plotted to their right (B, D, F, and H respectively).